ChemComm

Accepted Manuscript

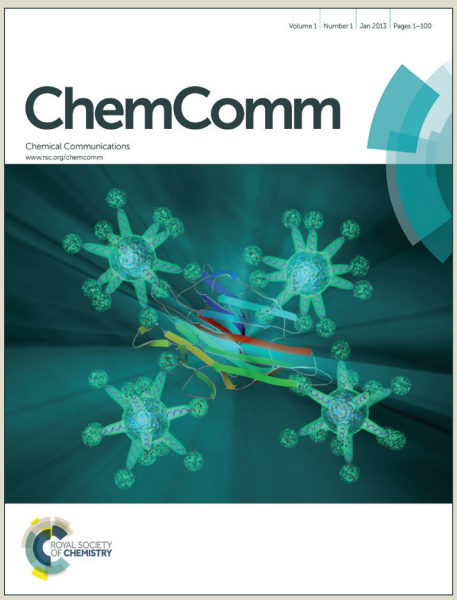

ROYAL SOCIETY OF CHEMISTRY

www.rsc.org/chemcomm

Journal Name

COMMUNICATION

Achieving High Power Efficiency and Low Roll-Off OLEDs Based on Energy Transfer from Thermally Activated Delayed Excitons to Fluorescent Dopants

Received 00th January 20xx,
Accepted 00th January 20xx

DOI: 10.1039/x0xx00000x

www.rsc.org/

Shipan Wang, Yuewei Zhang, Weiping Chen, Jinbei Wei, Yu Liu* and Yue Wang*

Achieving high power efficiencies at high-brightness levels is still an important issue for organic light-emitting diodes (OLEDs) based on thermally activated delayed fluorescence (TADF) mechanism. Herein, enhanced electroluminescence efficiencies were achieved in fluorescent OLEDs using a TADF molecule, (4s, 6s)-2,4,5,6-tetra(9H-carbazol-9-yl)isophthalonitrile (4CzIPN), as host and quinacridone derivatives (QA) as fluorescent dopants.

Enormous efforts have been made to develop high-efficiency organic light emitting devices (OLEDs) employing fluorescent or phosphorescent materials in the past decades.[1] According to spin statistics, conventional fluorescent OLEDs (FOLEDs) can only harvest 25% singlet excitons. Therefore, the maximum external quantum efficiency (EQE) is limited to 5% for common FOLEDs assuming a light-out-coupling efficiency of 20%. The internal electroluminescence efficiency (IQE) of 100% has been achieved in phosphorescent OLEDs (PHOLEDs) due to strong spin-orbit coupling of the heavy-metal center.[2] However, high costs, limited resources of phosphorescent materials and instability in blue PHOLEDs remain challenges for their application in long-term mass production for flat-panel displays and solid-state lighting.[3] Several approaches have been proposed to harvest the triplet excitons and improve the efficiency in FOLEDs.[4-9] Among them, FOLEDs based on thermally activated delayed fluorescence (TADF) mechanism have aroused researchers' great interest for their feasibility to achieve the IQE of 100% that is comparable with the best of PHOLEDs.[7-9] Generally, TADF molecules are employed as emitting materials in FOLEDs. To achieve efficient Dexter energy transfer (short-range electron-exchange energy transfer) from host to TADF molecules, the doping concentration of TADF molecules needs to be maintained at a relatively high level (5-10%). However, exciton quenching is quite significant at such a high doping concentration.[9] Therefore, the TADF emitter based OLEDs (TADF-emitter-OLEDs) often show serious efficiency roll-offs. To realize efficient transfer of all singlet and triplet energy from host to TADF dopant emitter, the band gap of the host molecule should be large enough to meet the demand that triplet energy of host molecule is larger than that of TADF dopant. Since the energy gap of the singlet-triplet splitting (ΔE_{ST}) is over 0.5 eV for most organic materials, the hosts of TADF materials usually have relatively deeper HOMO energy level and shallower LUMO energy level, which is not facile for the injection and transfer of hole or electron carriers in the emitting layer.[10] As a result, the TADF-emitter-OLEDs usually need higher driving voltages to overcome the energy barriers for holes or electrons injection. And this explains why most TADF-emitter-OLEDs display very high IQE but low power efficiencies (PE) at high brightness. Overall, for good performance at high-brightness levels, it is still a challenge to reduce the efficiency roll-offs in the TADF-emitter-OLEDs.

In this work, high-efficiency yellow-greenish FOLEDs with Commission International de l'Eclairage (CIE) coordinate of (0.44, 0.55) were developed based on the TADF mechanism. A typical TADF molecule, (4s, 6s)-2,4,5,6-tetra(9H-carbazol-9-yl)isophthalonitrile (4CzIPN)[7a] and quinacridone derivatives (QA) were used as host and fluorescent dopants, respectively (**Fig. 1**). Triplet excitons generated on 4CzIPN can be upconverted to its singlets by reverse intersystem crossing (RISC), and then transferred to the singlets of QA via a Förster energy transfer process. N,N'-di(n-butyl)-2,9-difluoroquinacridone (C_4-DFQA)[11] and N,N'-di(n-butyl)-1,3,8,10-tetrakis(trifluoromethyl)-quinacridone (C_4-TCF$_3$QA) with high photoluminescence (PL) quantum efficiency (Φ_{PL}) and good thermal stability (**Fig. S1 and S2**), were selected as guest

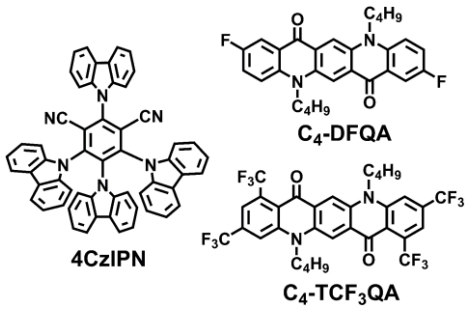

Fig. 1 Molecular structures of 4CzIPN, C_4-DFQA and C_4-TCF$_3$QA.

State Key Laboratory of Supramolecular Structure and Materials, College of Chemistry, Jilin University, Changchun 130012, P. R. China. E-mails: yuliu@jlu.edu.cn (Y. Liu); yuewang@jlu.edu.cn (Y. Wang); Fax: +86-431-85193421; Tel: +86-431-85168484.

Electronic Supplementary Information (ESI) available: [Experimental procedures, characterization data, and additional spectra]. See DOI: 10.1039/x0xx00000x

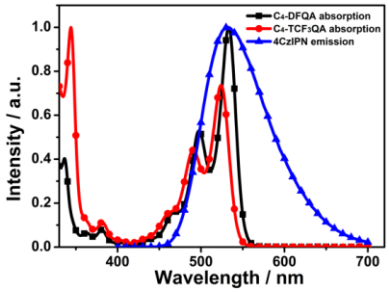

Fig. 2 The emission spectrum of 4CzIPN and the absorption spectra of C_4-DFQA and C_4-TCF_3QA measured in dilute dichloromethane solution (10^{-5} mol L^{-1}).

molecules. The theoretically calculated molecular orbital distributions of C_4-DFQA and C_4-TCF_3QA were shown in **Fig. S3**. The HOMO and LUMO orbitals of the two compounds distributed on the whole π-conjugated framework.

The UV/Vis spectra of C_4-DFQA and C_4-TCF_3QA in dilute CH_2Cl_2 solution were shown in **Fig. 2**, with the PL spectrum of 4CzIPN in CH_2Cl_2 for comparison. Intense absorption bands centering at 530 nm for C_4-DFQA and 525 nm for C_4-TCF_3QA were observed, which overlapped the PL spectrum of 4CzIPN well, suggesting efficient Förster energy transfer from 4CzIPN to QA derivatives. The PL spectra of 4CzIPN:C_4-DFQA and 4CzIPN:C_4-TCF_3QA films at different doping concentrations were also measured (**Fig. 3a** and **Fig. S4a**). At a low doping concentration of 0.5%, the PL spectra were dominated by the dopants' emission, which confirmed the effective energy transfer from 4CzIPN to QA derivatives. The maximum Φ_{PL} of 0.78 for 4CzIPN:C_4-DFQA and 0.82 for 4CzIPN:C_4-TCF_3QA was achieved at a 0.5% doping concentration (**Table S1**). To better understand the relationship between the excited states of the host and guest molecules, the transient PL characteristics of the doped films were analysed, with a Alq_3 (tris(8-hydroxyquinoline)aluminium):0.5% C_4-DFQA doped film for comparison. Two exponential decays with a prompt fluorescence decay of 22 ns and a delayed fluorescence decay of 0.84 μs in the time range of 5 μs were clearly observed in 4CzIPN:0.5% C_4-DFQA doped film, while there was only a prompt decay of 17 ns observed in Alq_3:0.5% C_4-DFQA cdoped film (**Fig. 3b**). The delayed fluorescence in an emitter using a TADF host should be attributed to the dopants' emission originated by energy transfer from the up-converted 4CzIPN triplets. In comparison with the delayed lifetime of ca. 5 μs of 4CzIPN reported in recent literatures,[7a] the TADF lifetime of the doped film greatly shortened, indicating rapid energy transfer from TADF host to the fluorescent dopants.[12-13] As revealed by previous studies, decreasing the triplet exciton lifetime is advantageous for the reduction of triplet-triplet annihilation (TTA) which mainly causes efficiency roll-off in TADF-emitter-OLEDs.[9g] To further confirm that the delayed fluorescence originated from TADF rather than other processes like TTA, we conducted the temperature-dependence of the transient PL experiment. As shown in **Fig. 3c**, the ratio of delayed components gradually increased with the temperature increasing from 100 K to 300 K. This is due to the acceleration of the RISC rate from triplet to singlet excited states by heat activation.[7] To study the photo-induced energy transfer process, we examined concentration-

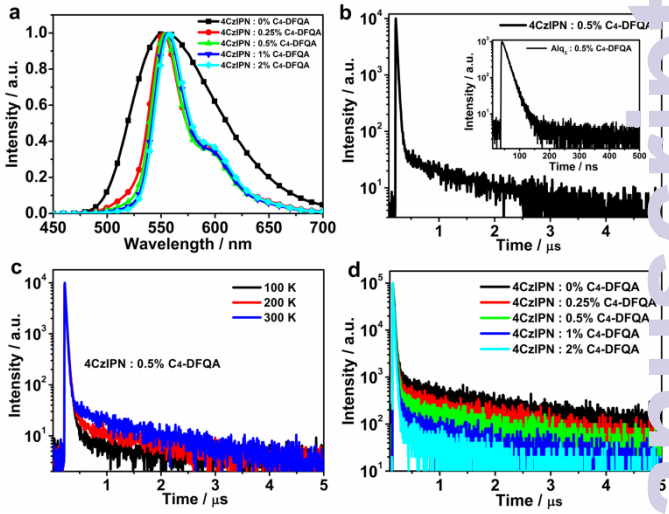

Fig. 3 a) The PL spectra of the 4CzIPN:C_4-DFQA films. b) The PL transient decay curves of the 4CzIPN:0.5 wt% C_4-DFQA and Alq_3:0.5 wt% C_4-DFQA (inset) film observed at 552 nm. c) Temperature-dependence of the transient PL spectra of the 4CzIPN:0.5 wt% C_4-DFQA film. d) The dopant concentration dependent PL transient decay curves of the 4CzIPN:C_4-DFQA films observed at 552 nm.

dependent transient behaviors (**Fig. 3d** and **Fig. S4b**). Upon increasing the doping concentration, the delayed lifetime and ratio of the delayed components were gradually reduced, indicating that the energy transfer process was accelerated, as evidenced in previous reports.[13-14] In the case of optical excitation, the triplet excitons in 4CzIPN were generated via ISC by singlet excitons, then transferred to the dopants' singlet state via RISC and Förster energy transfer processes. Finally, light was emitted as fluorescence from the singlet state of the dopants. The energy transfer rate can be accelerated by increasing the doping concentrations, ensuring efficient energy transfer between the host and the guest. But concentration quenching or Dexter energy transfer from host to guest that would result in efficiency loss at high doping concentration may be unavoidable. So the ideal doping concentration needs to be optimized by balancing the two factors.

The molecular structure of 4CzIPN was determined by single-crystal X-ray crystallographic analysis (**Fig. 4**). The twist angle between four carbazole units and the benzene ring were measured to be 59.5°, 55.6°, 61.8° and 56.7°, respectively. The highly twisted structure effectively reduced the π conjugation between the electron donor and acceptor units. The intermolecular π-π interaction was formed between the carbazole units which sandwiched in the two cyano groups with a contact distance of 3.4

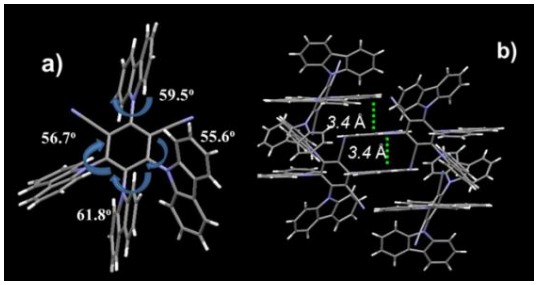

Fig. 4 Single crystal structure of 4CzIPN: molecular structure (a) and packing structure (b).

Å. The intermolecular aromatic stacking could offer a charge-transfer pathway and enhance carrier-transport ability, which is essential for excellent host materials.[15] To evaluate the carrier transporting properties of 4CzIPN host, single-carrier devices were fabricated. As shown in hole-only and electron-only device data in **Fig. S5**, the hole current density was similar to electron current density, indicating that the 4CzIPN host material possessed bipolar charge transport property and was effective to balance holes and electrons in the emitting layer. The time-of-flight (TOF) technique was also utilized to measure the carrier mobility of 4CzIPN (**Fig. S6**). The similar values of hole (μ_h) and electron (μ_e) mobility mean balanced charge transmission which is beneficial to improve device performance.[16] This feature also suggests that 4CzIPN can act as a bipolar host material.

To investigate the impact of this triplet harvesting process on TADF-host-FOLEDs performance, we fabricated the OLED devices with a structure of [ITO/NPB (35 nm)/mCP (5 nm)/emitter layer (EML) (30 nm)/BCP (5 nm)/$BePP_2$ (40 nm)/LiF (0.5 nm)/Al (150 nm)], with EMLs of 4CzIPN:0.5 wt% C_4-DFQA and 4CzIPN:0.5 wt% C_4-TCF_3QA, respectively. For comparison, devices with EMLs of Alq_3:0.5 wt% C_4-DFQA and Alq_3:0.5 wt% C_4-TCF_3QA were also fabricated, where Alq_3 was used as a conventional host. Here, we used NPB (1,4-bis[(1-naphthylphenyl)amino]-biphenyl) as the hole-transporting layer (HTL), mCP (1,3-bis(N-carbazolyl)benzene) as the exciton-blocking layer (EBL), BCP (2,9-dimethyl-4,7-diphenyl-1,10-phenanthroline) as the hole-blocking layer (HBL), $BePP_2$ (bis[2-(2-hydroxyphenyl)-pyridine]beryllium)[17] as the electron-transporting layer (ETL). The energy-level diagram of the devices and molecular structures of the used materials were shown in **Fig. S7**. The HOMO and LUMO energy levels of 4CzIPN, C_4-DFQA and C_4-TCF_3QA were calculated from the onsets of the oxidation and reduction potentials, respectively, according to the cyclic voltammetry measurements (**Fig. S8**). The electroluminescence (EL) characteristics of the devices were shown in **Fig. 5** and **Fig. S9**. The TADF-host-FOLEDs showed the maximum EQEs of 13.5% and 14.6%, respectively, much higher than those of the control devices using traditional Alq_3 host with maximum EQEs of ca. 5%. Obviously, those high EQE values broke through the theoretical limits for conventional FOLEDs, demonstrating that this process was effective for triplet harvesting by conventional fluorescent emitters. The performances of the devices were summarized in **Table 1**. As shown in **Fig. 5d**, 4CzIPN:0.5 wt% C_4-DFQA based device exhibited yellow-greenish emission, and the CIE coordinate of (0.44, 0.55) remained almost unchanged over a wide range of driving voltage, indicating efficient energy transfer. Despite a large hole-injection barrier of about 0.5 eV from NPB to mCP, the device exhibited a low turn-on voltage of 2.7 V. The maximum current efficiency (CE) of 48.9 cd A^{-1} and power efficiency (PE) of 53.4 lm W^{-1} were achieved without any light out-coupling enhancement, which are among the best values for FOLEDs with similar spectra. It's worth noting that the device showed a relatively small EQE roll-off at high brightness. The EQE of the device remained 12.6% at 1000 cd m^{-2} and 11.0% at 5000 cd m^{-2}, corresponding to 93% and 81% of the maximum EQE, respectively. And 4CzIPN:0.5 wt% C_4-TCF_3QA based device showed a similar performance (**Fig. S9**). It turned on at 2.8 V. The maximum CE and PE can be up to 48.0 cd A^{-1} and 46.1 lm W^{-1}, respectively.

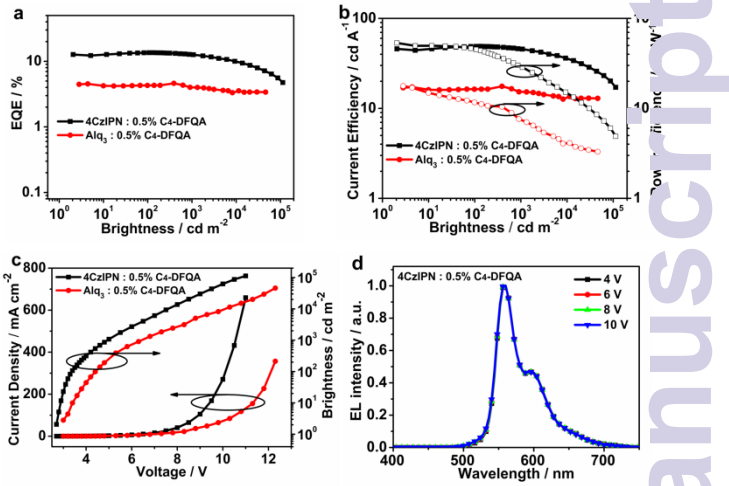

Fig. 5 The EL characteristics of devices based on C_4-DFQA. a) External quantum efficiency versus brightness characteristics. b) Current efficiencies and power efficiencies versus brightness characteristics. c) Current density–voltage–brightness (*J*–*V*–*L*) characteristics. d) The EL spectra operated at different voltages of the device.

Furthermore, high EQEs of 13.7% and 12.3% were achieved at 1[illegible] cd m^{-2} and 5000 cd m^{-2}, corresponding to 94% and 84% of th[illegible] maximum EQE, respectively, indicating a particularly sma[illegible] efficiency roll-off. The obtained efficiency roll-offs were much low[illegible] than those of the TADF-emitter-OLEDs reported recently.[9] One [illegible] the possible reasons for the low efficiency roll-offs is the suppression of the exciton annihilation due to the reduced tripl[illegible] exciton lifetime as mentioned above.[10] Besides, the bipolar charge transport property of 4CzIPN is effective to balance holes an[illegible] electrons in the emitting layer and guarantees a wide charge recombination region which could suppress the triplet-tripl[illegible] annihilation (TTA). Moreover, there are large energy barriers of 1.0 eV for electron leakage from 4CzIPN to mCP (T_1=2.9 eV) and 0.6 e[illegible] for hole leakage from 4CzIPN to BCP (T_1=2.8 eV), respectively. Efficient confinement of charges and triplet excitons within th[illegible] emitting layers contributes to the improvement of quant[illegible] efficiency and reduced efficiency roll-off at high brightness.[18] However, the large energy barriers also cause a higher roll-off in power efficiency than in EQE, such as 53.4 lm W^{-1} (maximum) to 3[illegible] lm W^{-1} at 1000 cd m^{-2}. And we believe that this may be furth[illegible] improved by carefully choosing the exciton-blocking materials. The EQE of OLEDs is described by the well-known equation of EQE = (γ [illegible] $\eta_\gamma \times \Phi_{PL}$) × η_{out}, where η_{out} is the light-out-coupling efficiency (c[illegible] 20%), γ is the recombination efficiency of injected holes an[illegible] electrons (ca. 100%), η_γ is efficiency of radiative exciton productio[illegible] (25% for conventional FOLEDs) and Φ_{PL} is 0.78 for 4CzIPN:0.5 wt[illegible] C_4-DFQA film and 0.82 for 4CzIPN:0.5 wt% C_4-TCF_3QA film. Thus, the η_γ values of C_4-DFQA and C_4-TCF_3QA devices can be estimated a[illegible] 87% and 89%, respectively. These results clearly indicate that th[illegible] devices overcome the theoretical limit of radiative exciton ratio [illegible] 25% for the conventional FOLEDs. In case of the excess excitor[illegible] produced by TTA, we examined the current density dependence o[illegible] the luminance experiment. The current density luminanc[illegible] increased linearly with an increase in current density (**Fig. S10**[illegible] suggesting that the high radiative exciton ratios originated from TADF rather than TTA.[9d]

In conclusion, we have successfully developed a kind of FOLEDs

Table 1. Electroluminescent properties of the devices.[a)]

Device	V_{on}/V	L_{max}/cd m^{-2}	PE_{max}/lm W^{-1}	EQE_{max}/%	PE[b)]/lm W^{-1}	EQE[b)]/%	CIE (x, y)[c)]
0.5% C_4-DFQA:4CzIPN	2.7	113,100	53.4	13.5	30.0, 18.5	12.6, 11.0	0.44, 0.55
0.5% C_4-TCF_3QA:4CzIPN	2.8	106,200	46.1	14.6	25.7, 16.9	13.7, 12.3	0.45, 0.54
0.5% C_4-DFQA:Alq_3	3.0	46,140	11.6	4.3	7.5, 4.9	4.0, 3.6	0.43, 0.55
0.5% C_4-TCF_3QA:Alq_3	3.0	50,240	12.5	4.6	8.6, 5.3	4.5, 3.9	0.43, 0.55

[a)] Abbreviation: V_{on}: Turn-on voltage. L_{max}: Maximum luminance. PE: The maximum power efficiency. EQE: The maximum external quantum efficiency. [b)] Values at 100 and 5000 cd m^{-2}. [c)] Measure at 100 cd m^{-2}.

with low driving voltages, high power efficiencies and low EQE roll-offs. Triplet excitons generated on the TADF host can be harvested by conventional fluorescent dopants via RISC and Förster energy transfer process. The TADF host based FOLEDs exhibit excellent performance with a maximum EQE of 13.5% and PE of 53.4 lm W^{-1}, which are two or three times higher than the best values of conventional FOLEDs. Moreover, the device maintains a high EQE of 12.6% at a practical brightness of 1000 cd m^{-2}, indicative of a low efficiency roll-off. This approach not only improves the efficiencies of conventional FOLEDs, but also reduces the efficiency roll-offs of TADF OLEDs. We believe our study will contribute to development of low-cost, high power efficiency, full-color and white TADF OLEDs.

This work was supported by the National Basic Research Program of China (2015CB655000), the National Natural Science Foundation of China (91333201 and 21221063) and Program for Chang Jiang Scholars and Innovative Research Team in University (No. IRT101713018).

Notes and references

1 a) J. E. Anthony, *Chem. Rev.*, 2006, **106**, 5028; b) A. C. Grimsdale, K. L. Chan, R. E. Martin, P. G. Jokisz and A. B. Holmes, *Chem. Rev.*, 2009, **109**, 897; c) L. Xiao, Z. Chen, B. Qu, J. Luo, S. Kong, Q. Gong and J. Kido, *Adv. Mater.*, 2011, **23**, 926.

2 a) M. A. Baldo, D. F. O'Brien, Y. You, A. Shoustikov, S. Sibley, M. E. Thompson and S. R. Forrest, *Nature*, 1998, **395**, 151; b) M. A. Baldo, S. Lamansky, P. E. Burrows, M. E. Thompson and S. R. Forrest, *Appl. Phys. Lett.*, 1999, **75**, 4; c) C. Adachi, M. A. Baldo, M. E. Thompson and S. R. Forrest, *J. Appl. Phys.*, 2001, **90**, 5048.

3 a) K. S. Yook and J. Y. Lee, *Adv. Mater.*, 2012, **24**, 3169; b) K. Sato, K. Shizu, K. Yoshimura, A. Kawada, H. Miyazaki and C. Adachi, *Phys. Rev. Lett.*, 2013, **110**, 247401.

4 M. A. Baldo, M. E. Thompson and S. R. Forrest, *Nature*, 2000, **403**, 750.

5 a) D. Kondakov, T. D. Pawlik, T. K. Hatwar and J. P. Spindler, *J. Appl.Phys.*, 2009, **106**, 124510; b) C. J. Chiang, A. Kimyonok, M. K. Etherington, G. C. Griffiths, V. Jankus, F. Turksoy and A. P. Monkman, *Adv. Funct. Mater.*, 2013, **23**, 739; c) J. -Y. Hu, Y. -J. Pu, F. Satoh, S. Kawata, H. Katagiri, H. Sasabe and J. Kido, *Adv. Funct. Mater.*, 2014, **24**, 2064.

6 a) W. J. Li, Y. Y. Pan, R. Xiao, Q. M. Peng, S. T. Zhang, D. G. Ma, F. Li, F. Z. Shen, Y. H. Wang, B. Yang and Y. G. Ma, *Adv. Funct. Mater.*, 2013, **24**, 1609; b) L. Yao, S. T. Zhang, R. Wang, W. J. Li, F. Z. Shen, B. Yang and Y. G. Ma, *Angew. Chem. Int. Ed.*, 2014, **53**, 2119; c) Y. Y. Pan, W. J. Li, S. T. Zhang, L. Yao, C. Gu, H. Xu, B. Yang and Y. G. Ma, *Adv. Opt. Mater.*, 2014, **2**, 510.

7 a) H. Uoyama, K. Goushi, K. Shizu, H. Nomura and C. Adachi, *Nature*, 2012, **492**, 234; b) K. Goushi, K. Yoshida, K. Sato and C. Adachi, *Nat. Photon.*, 2012, **6**, 253; c) J. Li, T. Nakagawa, J. Macdonald, Q. S. Zhang, H. Nomura, H. Miyazaki and C. Adachi, *Adv. Mater.*, 2013, **25**, 3319; d) F. B. Dias, K. N. Bourdakos, V. Jankus, K. C. Moss, K. T. Kamtekar, V. Bhalla, J. Santos, M. R. Bryce and A. P. Monkman, *Adv. Mater.*, 2013, **25**, 3707; e) Y. Tao, K. Yuan, T. Chen, P. Xu, H. Li, R. Chen, C. Zheng, L. Zhang and W. Huang, *Adv. Mater.*, 2014, **26**, 7931.

8 a) Q. S. Zhang, B. Li, S. P. Huang, H. Nomura, H. Tanaka and C. Adachi, *Nat. Photon.*, 2014, **8**, 326; b) B. S. Kim and J. Y. Lee, *Adv. Funct. Mater.*, 2014, **24**, 3970; c) C. W. Lee and J. Y. Lee, *Chem. Mater.*, 2014, **26**, 1413; d) Y. J. Cho, K. S. Yook and J. Y. Lee, *Adv. Mater.*, 2014, **26**, 4050; e) J. W. Sun, J. -H. Lee, C. -K. Moon, K. -H. Kim, H. Shin and J. -J. Kim, *Adv. Mater.,* 2014, **26**, 5684.

9 a) Q. Zhang, J. Li, K. Shizu, S. Huang, S. Hirata, H. Miyazaki and C. Adachi, *J. Am. Chem. Soc.*, 2012, **134**, 14706; b) G. Méhes, H. Nomura, Q. Zhang, T. Nakagawa and C. Adachi, *Angew. Chem. Int. Ed.*, 2012, **51**, 11311; c) H. Tanaka, K. Shizu, H. Miyazaki and C. Adachi, *Chem. Commun.*, 2012, **48**, 11392; d) T. Nakagawa, S. Y. Ku, K. T. Wong and C. Adachi, *Chem. Commun.*, 2012, **48**, 9580; e) H. Wang, L. Xie, Q. Peng, L. Meng, Y. Wang, Y. Yi and P. Wang, *Adv. Mater.*, 2014, **26**, 5198; f) S. Y. Lee, T. Yasuda, Y. S. Yang, Q. Zhang and C. Adachi, *Angew. Chem. Int. Ed.*, 2014, **53**, 6402; g) Q. Zhang, H. Kuwabara, W. J. Potscavage, S. Huang, Y. Hatae, T. Shibata and C. Adachi, *J. Am. Chem. Soc.*, 2014, **136**, 18070.

10 C. Murawski, K. Leo and M. C. Gather, *Adv. Mater.*, 2013, **25**, 6801.

11 a) Y. Zhao, X.M.C. Bao, Y. Fan, J. Zhang and Y. Wang, *Langmuir*, 2009, **25**, 3264; b) H. Bi, K. Ye, Y. Zhao, Y. Yang, Y. Liu and Y. Wang, *Org. Electron.*, 2010, **11**, 1180.

12 a) H. Nakanotani, T. Higuchi, T. Furukawa, K. Masui, K. Morimoto, M. Numata, H. Tanaka, Y. Sagara, T. Yasuda and C. Adachi, *Nat. Commun.*, 2014, **5**, 4016; b) T. Furukawa, H. Nakanotani, M. Inoue and C. Adachi, *Sci. Rep.*, 2015, **5**, 8429.

13 D. D. Zhang, L. Duan, C. Li, Y. L. Li, H. Y. Li, D. Q. Zhang and Y. Qiu, *Adv. Mater.*, 2014, **26**, 5050.

14 a) X. -K. Liu, Z. Chen, C. -J. Zheng, M. Chen, W. Liu, X. -H. Zhang and C. -S. Lee, *Adv. Mater.*, 2015, **27**, 2025; b) K. -H. Kim, C. -K. Moon, J. W. Sun, B. Sim and J. -J. Kim, *Adv. Opt. Mater.*, 2015, DOI: 10.1002/adom.201400644.

15 a) K. Wang, F. C. Zhao, C. G. Wang, S. Y. Chen, D. Chen, H. Y. Zhang, Y. Liu, D. G. Ma and Y. Wang, *Adv. Funct. Mater.*, 2013, **23**, 2672; b) K. Wang, S. P. Wang, J. B. Wei, S. Y. Chen, D. Liu, Y. Liu and Y. Wang, *J. Mater. Chem. C.*, 2014, **2**, 6817; c) K. Wang, S. P. Wang, J. B. Wei, Y. Miao, Y. Liu and Y. Wang, *Org. Electron.*, 2014, **15**, 3211.

16 D. D. Zhang, L. Duan, D. Q. Zhang, J. Qiao, G. F. Dong, L. D. Wang and Y. Qiu, *Org. Electron.*, 2013, **14**, 260.

17 a) Y. Liu, J. H. Guo, J. Feng, H. D. Zhang, Y. Q. Li and Y. Wang, *Appl. Phys. Lett.*, 2001, **78**, 2300; b) F. C. Zhao, Z. Q. Zhang, Y. P. Liu, Y. F. Dai, J. S. Chen and D. G. Ma, *Org. Electron.*, 2012, **13**, 1049.

18 S.-J. Su, E. Gonmori, H. Sasabe and J. Kido, *Adv. Mater.*, 2008, **20**, 4189.